Performance Validation of a Single-Tube Pulse Detonation Rocket System

doi: 10.2514/1.37924

Pre-print ver. (Kasahara, Hasegawa, Nemoto, Yamaguchi, Yajima, Kojima, JOURNAL OF PROPULSION AND POWER, Vol. 25, No. 1, January–February 2009)

Performance Validation of a Single-Tube Pulse Detonation Rocket System

Jiro Kasahara[*], Akira Hasegawa[†], Toyoshi Nemoto[†], Hiroyuki Yamaguchi[†]
University of Tsukuba, Tsukuba 305-8573, Japan

Takashi Yajima[‡]
IHI Aerospace Engineering, Tomioka 370-2307, Japan

and

Takayuki Kojima[§]
Japan Aerospace Exploration Agency, Chofu, 182-8522, Japan

Submitted April 7, 2008
Presented as Paper 5007 at the 43rd AIAA/ASME/SAE/ASEE Joint Propulsion Conference and Exhibit, Cincinnati, OH, 8-11 July 2007

Abstract

A pulse detonation engine (PDE) can be operated even if there are no compression mechanisms such as compressors or pistons, and a rocket engine with an extremely low combustor fill pressure (pulse detonation rocket, PDR) thus becomes possible. In this research, we made a model PDR system with increased specific impulse by partial fill. The performance predicted by this model was then confirmed experimentally. The thrust can be calculated by using the simplified PDE model of Endo et al. and the partial filling effect models of Sato et al. The mass flow rate of the propellant supplied from the pressurized cylinders is considered in this calculation. As a result, the thrust performance can be determined by the kind of propellant, the initial conditions of the gas in the cylinders, the supply-valve orifice and PDE-tube volume, and the operation frequencies. We fabricated a pulse detonation rocket (PDR) named “TODOROKI” and verified the thrust calculation model via a horizontal sliding test. We confirmed that the stability of the PDE operation depends on the ratio between the purge-gas thickness and the tube diameter. The thrust predicted by the model was identical to experimental results within 4%.

*Associate Professor, Department of Engineering Mechanics and Energy, Member AIAA

†Graduate Student, Department of Engineering Mechanics and Energy

‡Manager, Development Section No.1, Development Department

§Researcher, Institute of Space Technology and Aeronautics, Member AIAA

Nomenclature

A = orifice area

a = acceleration

D = Chapman-Jouguet velocity

D_{tube} = detonation tube diameter

d = equivalent valve orifice diameter

$\tilde{d}$ = actual valve orifice diameter

F = thrust

f = operation frequency

g = gravitational acceleration

I_{sp} = specific impulse

L_{tube} = detonation tube length

M = initial mass of a PDR system

m = mass of outflow gas

$\dot{m}$ = mass flow rate

N = number of parallel valves

p = pressure

R = gas constant

T = temperature

t = time

t_{Din} = input time of valve open to a sequencer

t_{Dout} = output time of valve open from a sequencer

t_{Oin} = input time of valve-open duration to a sequence

t_{Oout} = output time of valve-open duration from a sequencer

t_{Od} = delay time of valve open

t_{Cd} = delay time of valve close

t_{Pd} = time for valve-close process

t_{Dreal} = time between input and valve open times

t_{Oreal} = valve open time

u = velocity

υ = velocity
V = volume
$\dot{V}$ = volume flow rate
v = specific volume
x = position
γ = specific heat ratio
ε = valve-open time ratio
ε_p = purge-gas thickness ratio
η = effective efficiency of valve
μ = coefficient of static friction
μ' = coefficient of dynamic friction
ρ = density
σ^* = critical flow coefficient
ϕ = equivalence ratio
ψ = fill fraction

Subscripts

a = ambient gas
j = cycle number
d = propellant (fuel + oxidizer)
f = fuel
i = purge gas (inert gas)
o = oxidizer
t = PDE tube
cycle = PDE cycle
0 = initial condition

I. Introduction

A pulse detonation engine (PDE) [1, 2] obtains thrust by generating detonation intermittently. There are many PDE review papers (Kailasanath [3, 4], Bazhenova and Golub [5], Roy et al. [6]). The PDE for aerospace propulsion obtains thrust by blowing the detonated high-pressure gas down. The typical shape of a PDE is a straight tube. One end of this tube is closed, and the other is opened. After the tube is filled with propellant gas, the gas is ignited at the closed end of the tube and the detonation is initiated. A self-sustained detonation wave, which compresses the propellant by shock

waves, propagates toward the open end of the tube. A PDE can be operated even if there are no compression mechanisms such as compressors or pistons. Sufficient specific impulse (200-350 sec) can be obtained even by the same fill pressure as that of ambient air (Zitoun and Desbordes [7], Morris [8], Endo and Fujiwara [9], Endo et al. [10], Wintenberger et al. [11], Cooper et al. [12]), and thus a rocket engine with an extremely low combustor fill pressure (pulse detonation rocket, PDR) becomes possible [8]. The flow as a simplified PDE [9, 10] can be achieved because in the combustor of a PDR, there is no interaction with the air-breathing mechanism (intake and compressor) installed before the combustor. (The air-breathing PDE has been studied by many researchers: Tally and Coy [13], Wintenberger and Shepherd [14], Harris et al. [15], Ma et al. [16], Kojima and Kobayashi [17]). Moreover, it is easy to increase the specific impulse by using a mechanism (an extension tube for partial filling [18-21], a nozzle [8, 22-24], or an ejector [25, 26], or) installed after the combustor. The PDR obtains thrust consisting of the integration of small impulses. If we can control the timing of the impulse generation, we can achieve delicate thrust control.

Sato et al. [18] found that an increase in the specific impulse caused by the effect of partial fill was in inverse proportion to the square root of the ratio of the mass of the propellant to the mass of all gas (in the case that the fill pressure is equal to ambient pressure). Li and Kailasanath [19], Cooper et al. [20], and Endo et al. [21] also proposed partial-fill thrust models based on CFD, an experiment, and an energy-balance assumption, respectively. Morris [8] investigated thrust enhancement obtained by converging-diverging nozzles. Nozzle performance enhancement to a PDR, like steady flow, can be achieved when the ambient pressure is much lower than the initial pressure of the PDE tube. When the ambient pressure is extremely low, the specific impulse of the PDR is larger than that of the conventional rocket engine. Recently, Cooper and Shepherd [22] experimentally investigated the single-tube PDE with a nozzle, varying the ambient pressure from 1.4 to 100 kPa. They experimentally verified two regimes of nozzle operations. Cooper and Shepherd [23] also investigated the thrust of the straight tube PDE in sub-atmospheric pressure. Allgood et al. [24] measured the performance of the multi-cycle partial-fill PDE tube with nozzles. They experimentally investigated the relationship between partial fill fractions and nozzles. Kasahara et al. [27] performed experimental and numerical studies of the fundamental partial-fill effect by using an open shock tube. In the researches of Kasahara et al. [28, 29] and Hasegawa et al. [30], the PDR system experiments were performed, in which the combustor was partially filled with low-pressure propellant.

In the present paper, we proposed the PDR system model with the partial-fill effect. The performance predicted by this model was then confirmed experimentally. The thrust can be calculated by using the simplified PDE model of Endo et al. [10] and the partial filling effect models of Sato et al. [18]. In this paper, the mass flow rate of the propellant is also considered. The PDR

system performance can be determined by the kind of propellant, the initial conditions of the gas cylinders, the supply-valve orifice and PDE-tube volume, and the operation frequencies. We fabricated a pulse detonation rocket TODOROKI (PDR-TODOROKI) and verified the thrust model via a horizontal sliding test. PDR-TODOROKI has all the necessary components, such as the gas cylinders, electromagnetic valves, combustor (a PDE tube), and controller, and it can slide on the rails independently. PDR-TODOROKI has a spring-damper system that relaxes the intermittent impulsive thrust at the end wall of the PDE tube (combustor).

II. PDR Thrust Calculation

Figure 1 shows the system diagram of PDR-TODOROKI. The PDR is composed of three cylinders (for oxygen, ethylene, and helium gases), valves directly connected to the cylinders, a PDE tube (length L_{tube} and diameter D_{tube}), and an igniter. Figure 2 shows the operation sequence of the valves and the igniter. Both the fuel and oxidizer valves open and close simultaneously (open times of the fuel-oxidizer valves are $t_{\mathrm{open,f}}$ and $t_{\mathrm{open,o}}$, respectively), and subsequently the igniter operates, and the valve of the purge gas opens and closes after the detonation combustion (open times of the purge-gas valve is $t_{\mathrm{open,i}}$). The time period for one cycle is t_{cycle}. The thrust of PDR-TODOROKI can be determined from the volumes of the cylinders, the gaseous species, the initial gas states, the orifice diameters of the supply valves, the volume of the PDE tube, and the operation frequency. The mass flow rate of the gases, the equivalence ratio, the C-J velocity, and the fill fraction are parameters in this thrust calculation. It is assumed that the oxidizer and the purge gas are thermally perfect gas. It is also assumed that in the cylinder the fuel is liquid with constant equilibrium pressure, but outside of the cylinder the fuel is in the gas phase.

A. Mass Flow Rates of Propellants and Purge Gases

We calculated the mass flow rates of oxidizer and purge gas. Although the flow in the PDR supply system is not steady-state, the steady flow or no flow conditions are achieved by assuming that the operation time period of the PDR is sufficiently larger than both the characteristic time of flow (the cylinder length divided by the sonic speed of the gas) and valve-response time. In this calculation, we employed this assumption.

According to the finite cylinder volume, the pressure and mass flow rate in the cylinder decrease by outflow of the gas. By assuming the flow is isentropic, we obtained the mass flow rate as follows:

$$\dot{m} = \frac{\mathrm{d}m}{\mathrm{d}t} = \rho A \sigma^* \sqrt{RT_0} \left(\frac{\rho}{\rho_0} \right)^{\frac{\gamma-1}{2}} \tag{1}$$

where σ^* is the critical flow coefficient,

$$\sigma^* = \sqrt{\gamma \left(\frac{2}{\gamma+1} \right)^{\frac{\gamma+1}{\gamma-1}}} \tag{2}$$

If the outflow mass is identical to the decrease of mass in the cylinder, we obtain:

$$\mathrm{d}m = -V_0 \mathrm{d}\rho \tag{3}$$

Substituting Eq. (3) in Eq. (1) and integrating by time leads to the following equation:

$$\dot{m} = \delta \kappa \frac{p_0 V_0}{RT_0} \left\{ 1 + \frac{\gamma-1}{2} \delta \kappa t \right\}^{\frac{1+\gamma}{1-\gamma}} \tag{4}$$

where

$$\delta = \left(\frac{2}{\gamma+1} \right)^{\frac{\gamma+1}{2(\gamma-1)}}, \qquad \kappa = \frac{\pi \tilde{d}^2 \sqrt{\gamma RT_0}}{4V_0}$$

In this equation, $\tilde{d}$ is the equivalent valve orifice diameter. There is a relation between the valve open-time ratio $\varepsilon = t_{\mathrm{open}} / t_{\mathrm{cycle}}$, the effective valve efficiency η, the actual valve orifice diameter *d,* and the number of parallel valves *N*, as follows:

$$\frac{\pi \tilde{d}^2}{4} = \varepsilon \eta N \left(\frac{\pi d^2}{4} \right)$$

Therefore,

$$\widetilde{d} = d\sqrt{\varepsilon\eta N} \tag{5}$$

We can obtain mass flow rates of oxidizer $\dot{m}_{\mathrm{o}}$ and purge gas $\dot{m}_{\mathrm{i}}$ from Eq. (4).

According to the equilibrium pressure assumption, the fuel mass flow rate is expressed as follows:

$$\dot{m} = \delta\kappa\frac{pV}{RT} \tag{6}$$

B. Equivalence Ratio and Detonation Velocity of Propellants

The equivalence ratio of the propellant can be written by using the mass flow rate, as follows:

$$\phi = \frac{(F/O)}{(F/O)_{\mathrm{st}}} = \frac{\alpha_{\mathrm{o}}\dot{m}_{\mathrm{f}}R_{\mathrm{f}}}{\alpha_{\mathrm{f}}\dot{m}_{\mathrm{o}}R_{\mathrm{o}}} \tag{7}$$

where α is the stoichiometric coefficient.

The C-J velocity of propellant in the PDE tube $D(\phi)$ can be calculated using chemical equilibrium codes (AISTJAN [31]) by determining the equivalence ratio and the initial state of this propellant. In the case of calculating the ethylene-oxygen propellant, the equivalence ratio is given by $\phi = 3\dot{m}_{\mathrm{f}}R_{\mathrm{f}}/(\dot{m}_{\mathrm{o}}R_{\mathrm{o}})$. In such a case, the initial pressure and temperature were set to 0.1 MPa and 300 K, respectively.

C. Partial Fill Process in the PDE Tube

The fill fraction ψ of the propellant in the PDE tube is given by

$$\psi = \frac{V_{\mathrm{d}}}{V_{\mathrm{t}}} = \frac{\dot{V}_{\mathrm{d}}}{fV_{\mathrm{t}}} \tag{8}$$

where *f* is the operation frequency and V_{t} is the PDE tube volume. The volume flow rate $\dot{V}_{\mathrm{d}}$ is calculated as follows:

$$\dot{V}_{\mathrm{d}} = \dot{m}_{\mathrm{o}} v_{\mathrm{o}} + \dot{m}_{\mathrm{f}} v_{\mathrm{f}} = \dot{m}_{\mathrm{o}} \frac{R_{\mathrm{o}} T_{\mathrm{a}}}{p_{\mathrm{a}}} + \dot{m}_{\mathrm{f}} \frac{R_{\mathrm{f}} T_{\mathrm{a}}}{p_{\mathrm{a}}}$$

The propellant mass per one cycle m_{d} is given by

$$m_{\mathrm{d}} = \frac{\dot{m}_{\mathrm{o}} + \dot{m}_{\mathrm{f}}}{f} \tag{9}$$

The purge gas filled in the previous cycle (or the burned gas) exists in front of the propellant gas. This purge gas's volume V_{i} and mass m_{i} are calculated as follows:

$$\begin{aligned} V_{\mathrm{i}} &= (1-\psi) V_{\mathrm{t}} \\ m_{\mathrm{i}} &= \frac{p_{\mathrm{a}} V_{\mathrm{i}}}{R_{\mathrm{i}} T_{\mathrm{a}}} = (1-\psi) V_{\mathrm{t}} \frac{p_{\mathrm{a}}}{R_{\mathrm{i}} T_{\mathrm{a}}} \end{aligned} \tag{10}$$

In the first cycle, the PDE tube is filled with ambient air (not purge gas), and the air mass m_{a} is calculated as follows:

$$m_{\mathrm{a}} = (1-\psi) V_{\mathrm{t}} \frac{p_{\mathrm{a}}}{R_{\mathrm{a}} T_{\mathrm{a}}} \tag{11}$$

D. PDR Specific Impulse and Thrust

If the species and the initial states of gases in the PDE tube are determined, the specific impulse of the PDR can be a function of the equivalence ratio ϕ and the fill fraction ψ, as follows:

$$I_{\mathrm{sp}}(\phi, \psi)$$

There is a relationship between specific impulses of the full filling and detonation velocities, which can be expressed as

$$\frac{I_{\mathrm{sp}}(\phi, 1)}{I_{\mathrm{sp}}(1,1)} = \frac{D(\phi)}{D(1)} \tag{12}$$

In the case of ethylene-oxygen propellant, $I_{\mathrm{sp}}(1,1) = 171.2$ sec (Endo et al. [10]) and $D(1) = 2375.8$ m/s. From the semi-empirical formula of Sato et al. [18] and Eqs. (8)-(12), we obtained the following equation of the PDR specific impulse:

$$I_{\mathrm{sp}}(\phi,\psi) = \frac{I_{\mathrm{sp}}(\phi,1)}{\sqrt{Z}} = \frac{I_{\mathrm{sp}}(\phi,1)}{\sqrt{\dfrac{m_{\mathrm{d}}}{m_{\mathrm{d}}+m_{\mathrm{i}}}}} = I_{\mathrm{sp}}(\phi,1)\sqrt{1+\frac{fV_{\mathrm{t}}\dfrac{p_{\mathrm{a}}}{T_{\mathrm{a}}} - \dot{m}_{\mathrm{o}}R_{\mathrm{o}} - \dot{m}_{\mathrm{f}}R_{\mathrm{f}}}{R_{\mathrm{i}}(\dot{m}_{\mathrm{o}}+\dot{m}_{\mathrm{f}})}} \tag{13}$$

Please note that in our experiment, in the first cycle the inert gas was air (R_{i}=287.1 J/(kg K)) and that in the second and above cycles, the inert gas was helium (R_{i} = 2078 J/(kg K)). The PDR thrust can be calculated as follows:

$$F(\phi,\psi) = I_{\mathrm{sp}}(\phi,\psi)\ \left(\dot{m}_o + \dot{m}_f\right)g \tag{14}$$

E. PDR Motion on the Rail

The PDE sliding motion on the horizontal rail can be described as follows. When the initial PDR position and velocity are $x = 0$ and $\upsilon = 0$, we obtained the PDR acceleration a from the equation of motion,

$$a = \frac{F}{M - m_{\mathrm{f}} - m_{\mathrm{o}} - m_{\mathrm{i}}} - \mu' g \tag{15}$$

where M is the initial total mass of the PDR and μ is the coefficient of dynamic friction. The PDR velocity and position are written as $\upsilon = \int_0^t a\,\mathrm{d}t$ and $x = \int_0^t \upsilon\,\mathrm{d}t$, respectively.

The time-averaged quantity A in the cycle j is defined as $\overline{A}_{\mathrm{j}} = \dfrac{1}{t_{\mathrm{cycle}}}\int_{t_{\mathrm{j}}}^{t_{\mathrm{j}}+t_{\mathrm{cycle}}} A\,\mathrm{d}t$. By assuming the PDR mass and specific-impulse changes in one cycle are small and negligible, we can easily calculate the acceleration, velocity, and position in cycle j as follows:

$$\overline{a}_{\mathrm{j}} = \frac{gI_{\mathrm{sp,\,j}}}{M - m_{\mathrm{f,\,j}} - m_{\mathrm{o,\,j}} - m_{\mathrm{i,\,j}}} \overline{\dot{m}}_{j} - \mu g \ , \tag{16}$$

$$\upsilon_{\mathrm{j}} = \int_{0}^{t_{\mathrm{j}}+t_{\mathrm{cycle}}} a \mathrm{d}t = t_{\mathrm{cycle}} \sum_{\mathrm{k}=1}^{j} \overline{a}_{\mathrm{k}} \ , \tag{17}$$

$$x_{\mathrm{j}} = \int_{0}^{t_{\mathrm{j}}+t_{\mathrm{cycle}}} \upsilon \mathrm{d}t = t_{\mathrm{cycle}} \sum_{\mathrm{k}=1}^{j} \overline{\upsilon}_{\mathrm{k}} \tag{18}$$

where j is cycle number, and

$$\overline{\dot{m}}_{\mathrm{j}} = \frac{1}{t_{\mathrm{cycle}}} \int_{t_{\mathrm{j}}}^{t_{\mathrm{j}}+t_{\mathrm{cycle}}} (\dot{m}_{\mathrm{f,j}} + \dot{m}_{\mathrm{o,j}}) \mathrm{d}t = \frac{m_{\mathrm{d,j}}}{t_{\mathrm{cycle}}} \ . \tag{19}$$

F. PDR Thrust of the Ethylene-Oxygen Propellant

The thrust of the PDR was calculated in the ethylene-oxygen propellant case. Figure 3 shows the 3-sec. time-averaged thrust of the ethylene-oxygen PDR with the same PDE-tube volume (3.25 liter) as "TODOROKI". The equivalent valve-orifice diameters, d_{o} and d_{f}, and cylinder volume V_{o} are parameters in this figure.

The thrust curves in Fig. 3 have two gradients. The large-gradient curves are in the low operation-frequency region ($0 \le f \le 20\,\mathrm{Hz}$), while the small-gradient curves are in the high-frequency region ($f > 20\,\mathrm{Hz}$). In the low operation frequency, the PDR tube is fully filled with the propellant ($\psi \ge 1$). In this region a part of the propellant is in the PDE tube, but the other part of the propellant is in outside of the PDE tube. Therefore, this thrust is strongly dependent on the constant PDE-tube volume divided by the propellant volume in one cycle. Thus the PDR thrust is almost simply proportional to the frequency (cycle number/second) and this curve has larger gradient than in the high frequency region. In the high-frequency region, the PDR tube is partially filled ($\psi < 1$). The fill fraction decreases with an increase in the operation frequency, because the fill-propellant volume per cycle decreases. In this case, specific impulse increases according to Equation 13. In Equation 14, thrust is proportional to the increases of the specific impulse, when the mass flow rate is constant. Therefore, the thrust increase in this high-frequency region is caused by the effect of the partial fill.

In Fig. 3 the cylinder volumes are changed from 0.25 to 10 liters. The smaller-volume cylinder obtains a smaller time-averaged thrust, because the supply-pressure decrease is faster. If the orifice diameter is small, the dependence of cylinder volume on the thrust becomes small, while the time-averaged thrust is also small. We should determine the cylinder sizes by considering the required total operation time and the time-average thrust.

III. Experiments and Discussion

Figures 4 and 5 show the PDR-TODOROKI photograph and system diagram, respectively. the total length of the PDR is 2173 mm, the diameter of the cylindrical main body is 200 mm, and the total mass of the PDR is 24.1 kg. The PDR is composed of three parts: a control section inside a nose cone at the top of the PDR, a supply section consisting of four solenoid valves, and an engine section consisting of the PDE tube and a spring-damper mechanism. As shown in Fig. 5 seamless aluminum-alloy cylinders (Teinen Kogyo) of 0.48, 0.48, and 1.0 liter are filled with ethylene, oxygen, and helium, respectively. The stop valves (Daito Valve) of these cylinders have larger C_v values than those of the solenoid valves (CKD, A2-6311, A2-6312, C_v=0.071-0.101). The pressures inside these cylinders are measured by pressure gauges (PG-35H, Copal electronics), as shown in Fig. 5.

The control section of the PDR is composed of the nose-cone control unit, the external PC connected with this unit by the umbilical connector and the cables, and the valve-igniter system. This unit can control the valve-igniter system even if the umbilical connector comes off, because it has a built-in battery and CPU. The PDR is able to slide on the rail using its four wheels (MISUMI EKBH35) located at 345 and 1052 mm from the nose tip. The coefficients of static and dynamic frictions are as follows.

$$\mu = 0.06218, \qquad \mu' = 0.008059$$

As shown in Fig. 6 the engine section has an oscillation damping mechanism to protect the main body from a large-impulsive thrust generated by detonation combustion. The PDE tube in the engine section has a tapered tube and a cylindrical main tube. The other end of the PDE tube is open to the ambient air. The diameter and length of the cylindrical main tube are 800 and 70 mm, respectively (L_{tube}/D_{tube}=11.4). The full-opened angle of the tapered tube (120.7 mm length) is 30 degrees. The PDE tube inside volume, including the tapered part of the tube, is 3.25 liters. The automobile igniter (NGK 8HSA) is located on the tapered tube. The PDE tube is connected to the main body by slide guides (Misumi SSE2B) and a spring (k=1000 N/m). This connecting mechanism has a damping function. The top portion of the PDE tube has both injection and sliding functions, so the PDE tube is able to both oscillate and always be supplied with gases from the cylinders.

The PDR gliding tests were performed on a 9-m rail (channel steel). Thrust was determined from the second-order differential of gliding displacement from the initial location. The displacement was measured by a CCD video camera. The CCD video camera was located in the line perpendicular to and at 10-m distance from the rail. The drag force on the body from air was estimated to be of a 0.1 N order, which is much smaller than the thrust. Thus we ignored the drag force in this thrust calculation.

A. PDR Stationary Test

An accurate valve-response time and detonation initiation observations are necessary for achieving stable operation of the PDR. We performed a stationary test on the PDR, a schematic diagram of which is shown in Fig. 7. Only the PDE engine part (the PDE tube) was used in this test. The fuel, oxygen, and purge gas were supplied from external 47-liter cylinders. The electromagnetic-valve motion was observed by using the pressure gauges located upstream of the valves.

Figure 8 shows the valve sequence and idealized valve operation. Figure 9 shows the valve-open time dependency on upstream pressure of the valve. In Fig 8 the input and output sequences of the control section and the idealized valve operation (pressure before the valve) are shown. The valve-open time linearly increases with an increase in valve upstream pressure. If the valve upstream pressure becomes high, the valve-close response time, which is part of the valve-open time, becomes longer. In the present experiment, we introduce the valve effective efficiency by including this change of valve-open time [sec], as follows:

valve effective efficiency of oxygen valves : $\eta = 1 - 0.14t$

valve effective efficiency of helium valve : $\eta = 1 - 0.06t$

valve effective efficiency of ethylene valve : $\eta = 0.8$

The valve effective efficiencies are essentially changed by the primary pressure of the valves, which decreases with an increase in the time from the operation start. However, in the present experiment, the initial pressure and temperature of each cylinder is almost same in every shot. For simplicity, we express the valve effective efficiencies as only a liner function of the time from the operation start. These efficiencies were determined by the blow-down test for valves.

The detonation initiation and thrust generation were confirmed by using the explosion sensor and the laser displacement meter. The explosion sensor was positioned at 600 mm from the open-end point on the PDE-tube axis. This explosion sensor can measure the pressure of a shock wave generated from the PDE tube. It can also measure the arrival time of the shock wave. From these measurement results, we can obtain the criteria information regarding the detonation

initiation and obtain the initiation time. The laser displacement meter, which can detect the displacement of the PDE tube by using the laser reflection from the wedged reflection plate attached to the side of the PDE tube as shown in Fig. 7, can measure the slide distance of the PDE tube. From this measurement result, we can obtain the information regarding the thrust generation and its time.

Figures 10 and 11 show the stable-operation results. In Fig. 10 the igniter operation, the shock wave arrival, and the PDE-tube motion start are simultaneous. From these results we can confirm that a detonation initiation was successfully done at the PDE tube. Figure 11 shows the monitoring results of the valve and igniter operations.

Sakurai et al. [32] showed that the purge gas volume strongly affects the detonation initiation. We investigated the effect of purge gas on the detonation-initiation stability. The purge gas is the gas barrier between the fresh propellant mixture and the burned gas. As shown in Fig. 1, the purge-gas thickness ratio is defined by $\varepsilon_{\mathrm{p}} = L_{\mathrm{i}} / D_{\mathrm{tube}}$, where L_{i} is the purge thickness. Table 1 shows the detonation-initiation success rate in some experiments. The detonation-initiation success rate is defined by the successfully initiated detonation cycle number divided by the total cycle number. The detonation was initiated in all cycles when $\varepsilon_{\mathrm{p}} \geq 3.12$. As these results show, the detonation initiation depends on the purge-gas thickness or thickness ratio. This is because the diffusion between the purge gas and the other gases is strongly dominated by this purge-gas thickness or thickness ratio.

B. PDR Sliding Test

The experimental conditions of the sliding test were as follows. The ambient temperature was 284 K, the ambient pressure was 101.9 kPa, the PDR operation frequency was 6.667 Hz, the operation time duration was 3 sec, the total cycle number was 13, and the initial pressures of ethylene, oxygen, and helium were 5.2, 13.6, and 9.6 MPa, respectively. The sliding distance, velocity history, and thrust history are shown in Fig. 12, 13, and 14, respectively. In the present experiment, the main experimental error occurred in determining the position of the PDR by the CCD camera. The error bars shown in Figs 12-14 are due to the maximum spatial resolution error of $\pm 5\%$, which corresponds to ± 2 pixels of the CCD images. The actual PDR thrust is impulsive (a peak thrust is approximately 5000 N); therefore, we used a one-cycle-averaged thrust calculated by Equations 14 and 19 and shown in Fig. 14. The Table 2 shows the experimental results, calculated results, and their difference. The experimental results were identical to the calculation results to within 4%. In the first cycle, a large thrust was generated due to heavy purge gas of air. The equation of Sato et al. [18] can be used in a PDE where the purge-gas species varies from cycle to cycle. The slow decrease

of the thrust in Fig. 14 is due to the decrease of the oxygen tank fill pressure. This decrease of the pressure is included in the PDR model. The PDR stationary and sliding tests were performed three and two times, respectively, in the present experiment for checking the stable operation and the repeatability of the data. The other sliding test was successfully run and the 3-second time averaged thrust was 30.45 N .

Conclusion

We fabricated a pulse detonation rocket (PDR) named “TODOROKI” and verified the thrust calculation model using a horizontal sliding test. The thrust can be calculated by using the simplified PDE model of Endo et al. and the partial filling effect models of Sato et al. The mass flow rate of the propellant supplied from the pressurized cylinders was considered in this calculation. As a result, the thrust performance could be determined by the kind of propellant, the initial conditions of the gas in the cylinders, the supply-valve orifice and PDE-tube volume, and the operation frequencies. PDR-TODOROKI has all the necessary components such as the gas cylinders, electromagnetic valves, combustor (a PDE tube), and controller, and it can slide on the rails independently. PDR-TODOROKI has a spring-damper system that relaxes the intermittent impulsive thrust at the end wall of the PDE tube (combustor). We confirmed that the stability of the PDE operation depends on the ratio between the purge-gas thickness and the tube diameter. In the sliding test of the PDR-TODOROKI of 6.67-Hz operation frequency during 13 cycles, a maximum thrust of 42.1 N and a time-averaged thrust of 34.0 N were achieved. The thrust predicted by the calculation model was identical to the experimental results to within 4%.

Acknowledgement

This study was conducted as part of the “Development of the Next-Generation Aerospace Rocket Engine Using Pulse Detonation Engine Mechanism” program of Project Research (S) at the University of Tsukuba, managed by Prof. M. Murakami. This study was also partially supported by Industrial Research Grant Programs 2004-2007 from the New Energy and Industrial Technology Development Organization (NEDO) of Japan, and the study was also partially supported by Grants-in-Aid for Scientific Research, Encouragement of Young Scientists (B) 2005-2007 from the Japan Society for the Promotion of Science (JSPS). We express our thanks to Mr. F. Yamamoto, and to Mr. H. Tanaka of IHI Aerospace Engineering for their great contributions to our study.

References

[1] Nicholls, J. A., Wilkinson, H. R., and Morrison, R. B., "Intermittent Detonation as a Thrust-Producing Mechanism," *Jet Propulsion*, Vol. 27, 1957, pp. 534-541.

[2] Bussing, T. R. A., and Pappas, G., "Pulse Detonation Engine Theory and Concepts," *Developments in High-Speed-Vehicle Propulsion Systems, Progress in Astronautics and Aeronautics,* No. 165, AIAA, 1996, pp. 421-472.

[3] Kailasanath, K., "Review of Propulsion Applications of Detonation Waves," *AIAA Journal*, Vol. 38, No. 9, 2000, pp. 1698-1708.

[4] Kailasanath, K., "Recent Developments in the Research on Pulse Detonation Engines, *AIAA Journal*, Vol. 41, No. 2, 2003, pp. 145-159.

[5] Bazhenova, T. V., and Golub V. V., "Use of Gas Detonation in a Controlled Frequency Mode (review), *Combustion Explosion and Shock Waves,* Vol. 39, No. 4, 2003, pp. 365-381.

[6] Roy, G. D., Frolov, S. M., Borisov, A. A., and Netzer, D. W., "Pulse Detonation Propulsion: Challenges, Current Status, and Future Perspective," *Progress in Energy and Combustion Science*, Vol. 30, 2004, pp. 545-672.

[7] Zitoun, R., and Desbordes, D., "Propulsive Performance of Pulsed Detonations," *Combustion Science and Technology*, Vol. 144, 1999, pp. 93-114.

[8] Morris, C. I., "Numerical Modeling of Single-Pulse Gasdynamics and Performance of Pulse Detonation Rocket Engines," *Journal of Propulsion and Power*, Vol. 21, No. 3, 2005, pp. 527-538.

[9] Endo, T., and Fujiwara, T., "A Simplified Analysis on a Pulse Detonation Engine Model," *Transaction of the Japan Society for Aeronautical and Space Sciences*, Vol. 44, No. 146, 2002, pp. 217-222.

[10] Endo, T. Kasahara, J., Matsuo, A., Inaba, K., Sato, S., and Fujiwara, T., "Pressure History at the Thrust Wall of a Simplified Pulse Detonation Engine," *AIAA Journal*, Vol. 42, No. 9, 2004, pp. 1921-1929.

[11] Wintenberger, E., Austin, J. M., Cooper, M., Jackson, S., and Shepherd, J. E., "Analytical Model for the Impulse of Single-Cycle Pulse Detonation Tube," *Journal of Propulsion and Power,* Vol. 19, No. 1, 2003, pp. 22-38.

[12] Cooper, M., Jackson, S., Austin, J., Wintenberger, E., and Shepherd, J. E., "Direct Experimental Impulse Measurements for Detonations and Deflagrations," *Journal of Propulsion and Power* Vol. 18, No. 5, 2002, pp. 1033-1041.

[13] Talley, D. G., and Coy E. B., "Constant Volume Limit of Pulsed Propulsion for a Constant γ Ideal Gas," *Journal of Propulsion and Power,* Vol. 18, no. 2, 2002, pp. 400-406.

[14] Wintenberger, E., and Shepherd, J. E., "Model for the Performance of Airbreathing Pulse-Detonation Engine," *Journal of Propulsion and Power,* Vol. 22, No. 3, 2006, pp. 593-603.

[15] Harris, P. G., Stowe, R. A. Ripley, R. C., and Guzik, S. M., "Pulse Detonation Engine as a Ramjet Replacement," *Journal of Propulsion and Power*, Vol. 22, No. 2, 2006, pp. 462-473.

[16] Ma, F., Choi, J.-Y., and Yang, V., "Propulsive Performance of Airbreathing Pulse Detonation Engines," *Journal of Propulsion and Power*, Vol. 22, No. 6, 2006, pp.1188-1203.

[17] Kojima, T, and Kobayashi, H., "Thrust Increase of Air Breathing Pulse Detonation Engine by High Supply Pressure," *Space Technology Japan*, Vol. 4, 2005, pp. 35-42.

[18] Sato, S., Matsuo, A., Endo, T., and Kasahara, J., "Numerical Studies on Specific Impulse of Partially Filled Pulse Detonation Rocket Engines," *Journal of Propulsion and Power*, Vol. 22, No. 1, 2006, pp. 64-69.

[19] Li, C. and Kailasanath, K., "Performance Analysis of Pulse Detonation Engines with Partial Fuel Filling," *Journal of Propulsion and Power*, Vol. 19, No. 5, 2003, pp. 908-916.

[20] Cooper, M., Shepherd, J. E., and Schauer, F., "Impulse Correlation for Partially Filled Detonation Tubes," *Journal of Propulsion and Power*, Vol. 20, No. 5, 2004, pp. 947–950.

[21] Endo, T., Yatsufusa, T., Taki, S., Matsuo, A., Inaba, K., and Kasahara, J., "Homogeneous-Dilution Model of Partially-Fueled Simplified Pulse Detonation Engines," Journal of Propulsion and Power, Vol. 23, No. 5, 2007, pp. 1033–1041.

[22] Cooper, M., and Shepherd, J. E., "Single-Cycle Impulse from Detonation Tubes with Nozzles, " *Journal of Propulsion and Power*, Vol. 24, No. 1, 2008, pp. 81-87.

[23] Cooper, M., and Shepherd, J. E., "Detonation Tube Impulse in Subatmospheric Environments," *Journal of Propulsion and Power*, Vol. 22, No. 4, 2006, pp. 845–851.

[24] Allgood, D., Gutmark, E., Hoke, J., Bradley, R., and Schauer, F., "Performance Measurements of Multicycle Pulse-Detonation-Engine Exhaust Nozzles," *Journal of Propulsion and Power*, Vol. 22, No. 1, 2006, pp. 70–77.

[25] Wilson, J., Sgondea, A., Paxson, D. E., and Rosenthal, B. N., "Parametric Investigation of Thrust Augmentation by Ejectors on a Pulsed Detonation Tube," *Journal of Propulsion and Power*, Vol. 23, No. 1, 2007, pp. 108-115.

[26] Wilson, J., "Effect on Pulse Length and Ejector Radius on Unsteady Ejector Performance," *Journal of Propulsion and Power*, Vol. 23, No. 2, 2007, pp. 345-352.

[27] Kasahara, J., Liang, Z., Browne, S. T., and Shepherd, J. E., "Impulse Generation by an Open Shock Tube," *AIAA Journal*, Vol. 46. No.7, July 2008, pp.1593-1603.

[28] Kasahara, J., Hirano, M., Matsuo, A., Sato, S., Endo, T., and Satori, S. "Flight Experiments Regarding Ethylene-Oxygen Single-Tube Pulse Detonation Rocket," AIAA Paper 2004-3918, 2004 July.

[29] Kasahara, J., "Pulse Detonation Rockets and Thrust Augmentation According to Partially-Filling Effect," *Journal of the Combustion Society of Japan*, Vol. 47, No. 140, 2005, pp. 84-89.

[30] Hasegawa, A., Nemoto, T., Yamaguchi, H., Kasahara, J., Yajima, T., Yamamoto, F., Tanaka, H., and Kojima, T., "Thrust Demonstration of a Pulse Detonation Rocket System for Flight Test," *The 47th Conference on Aerospace Propulsion and Power*, 2007 March, pp. 399-404.

[31] Tanaka, K., AISTJAN, http://www.aist.go.jp/RIODB/ChemTherm/gas.htm

[32] Sakurai, T., Ooko, A., Yoshihashi T., Obara T., and Ohyagi S., "Investigation of the Purge Process on the Multi-Cycle Operations of a Pulse Detonation Engine," *Transaction of the Japan Society for Aeronautical and Space Sciences*, Vol. 48, No. 160, 2005, pp. 78-85.

Table 1 Detonation initiation success rate in the PDR stationary test

Shot number	Ethylene supplying pressure	Oxygen supplying pressure	Helium supplying pressure	Propellant volume	Helium volume
	Pe	Po	Pi	Vd	Vi
	[MPa]	[MPa]	[MPa]	[L/cycle]	[L/cycle]
1	2.1	4.5	4.5	0.76	0.47
2	7	10	6	2	0.63
3	1.5	4	8	0.62	0.84
4	6.5	8	10	1.73	1.05
5	7	13	13	2.31	1.36

Shot number	Equivalence ratio	Volume ratio	Purge length	Purge thickness ratio	Success rate
	φ	Vi/Vd	Li	Li/Dtube	
			[m]		
1	1.92	0.62	0.12	1.74	4/5
2	2.87	0.32	0.16	2.34	4/5
3	1.54	1.35	0.22	3.12	5/5
4	3.33	0.61	0.27	3.9	5/5
5	2.21	0.59	0.35	5.05	5/5

Table 2 PDR sliding test results

	Experiment	Calculation	Difference
Maximum thrust	42.1 [N]	42.7 [N]	-1.45 [%]
Minimum thrust	29.7 [N]	30.7 [N]	-2.12 [%]
2-second time-averaged thrust	34.0 [N]	34.7 [N]	-2.21 [%]
Maximum speed	2.65 [m/s]	2.73 [m/s]	-3.02 [%]
Total sliding distance	2.87 [m]	2.98 [m]	-3.83 [%]

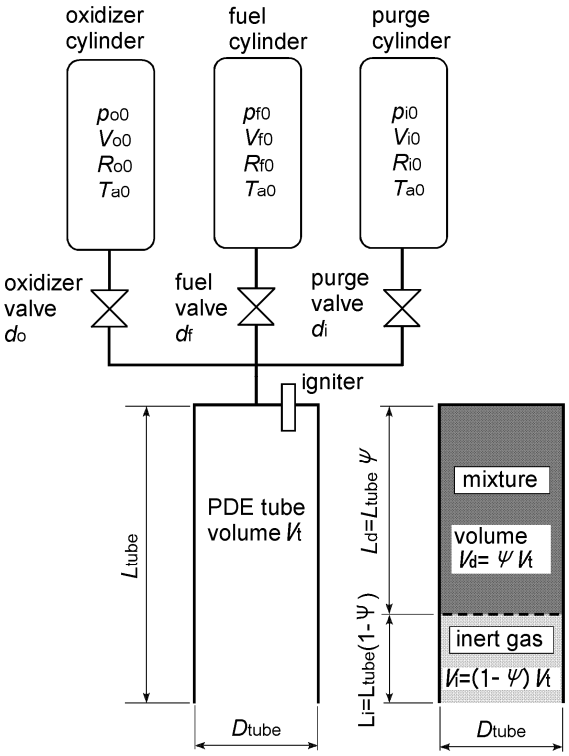

Fig.1 PDR-TODOROKI system diagram

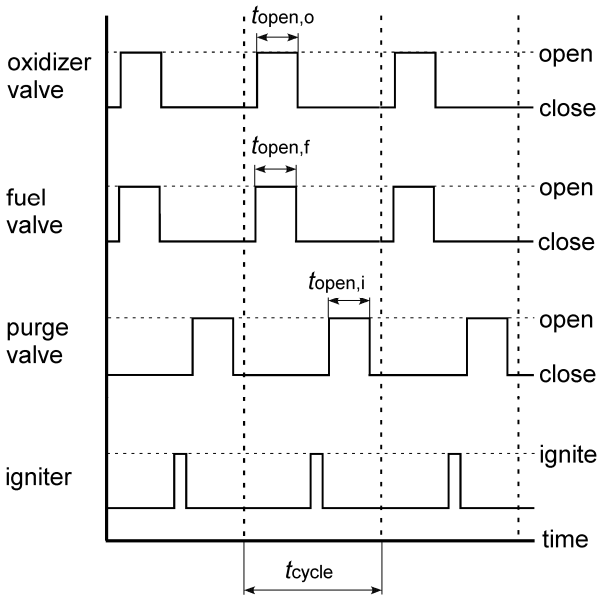

Fig.2 Valve-igniter operation sequence

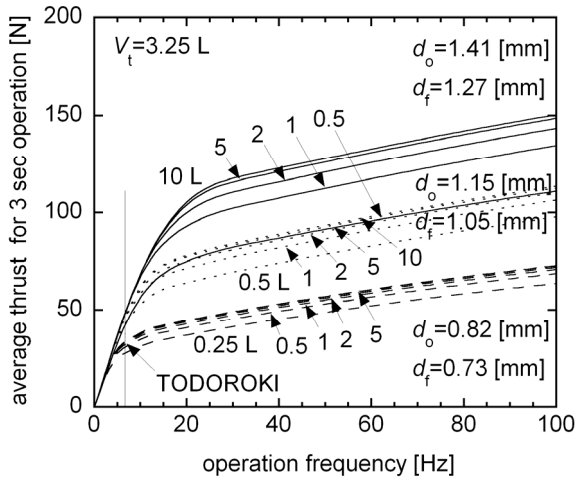

Fig.3 Time-averaged thrust of ethylene-oxygen PDR

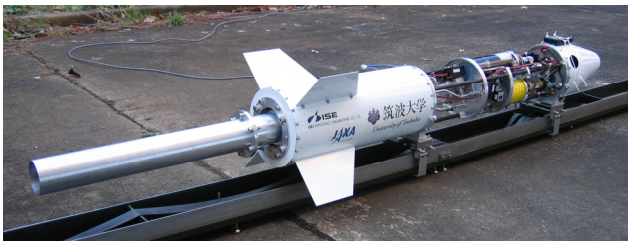

Fig.4 Pulse detonation rocket TODOROKI

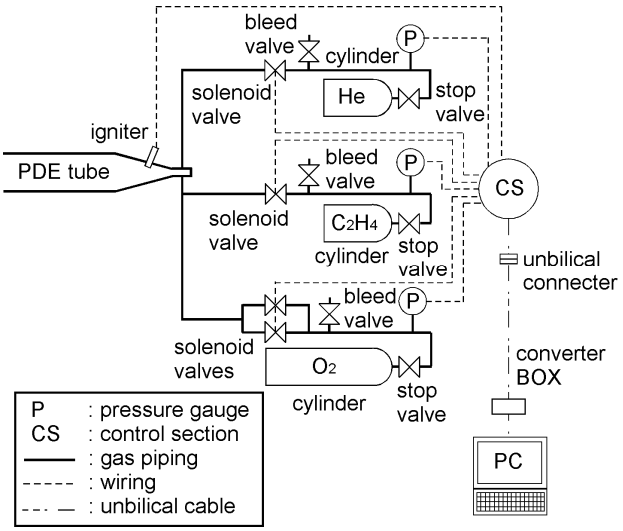

Fig.5 System diagram of PDR-TODOROKI

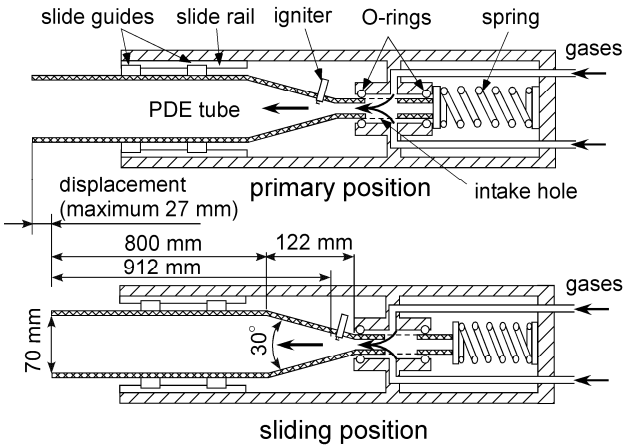

Fig.6 Thrust damping mechanism of PDR-TODOROKI

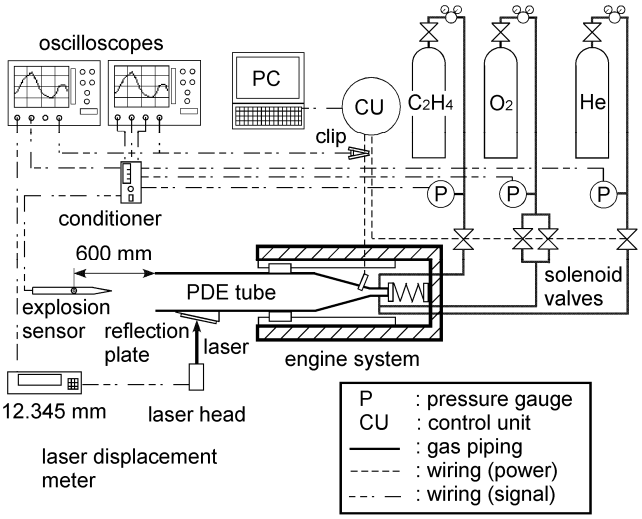

Fig.7 Schematic diagram of the PDR stationary test

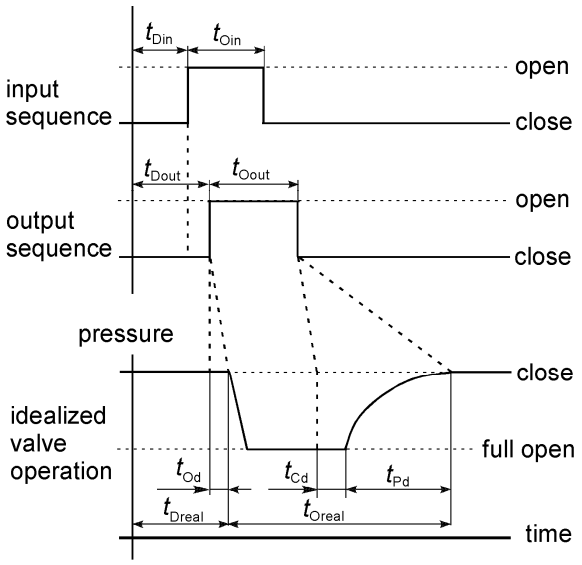

Fig.8 Valve sequence and idealized valve operation

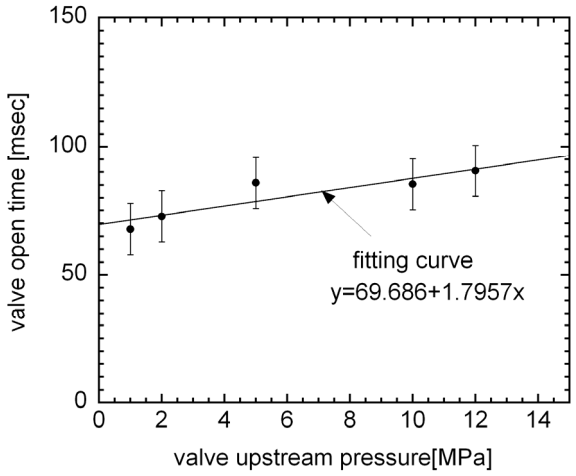

Fig.9 Valve-open time dependency on the upstream pressure

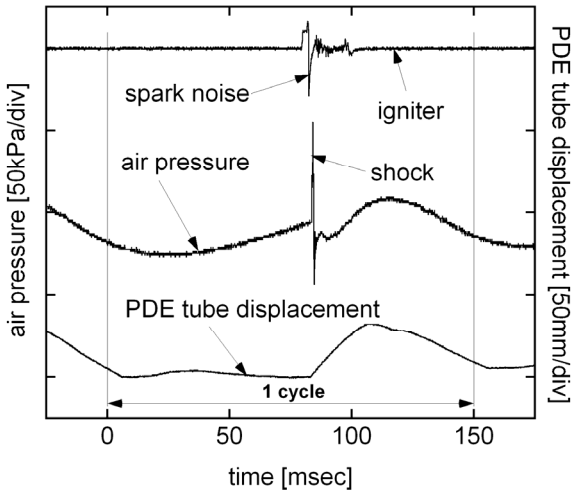

Fig.10 Stable-detonation-initiation monitoring results

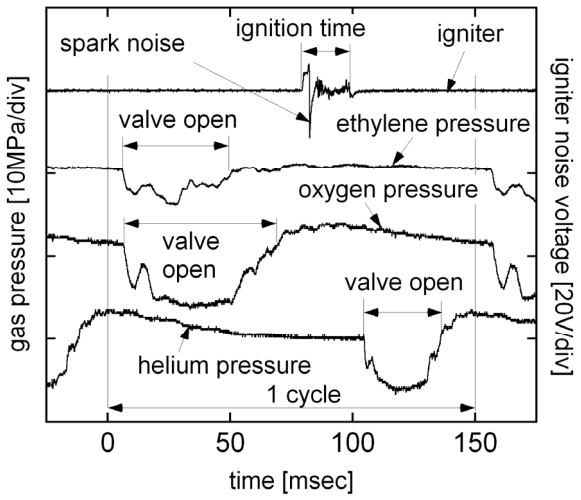

Fig.11 Valve operation monitoring results

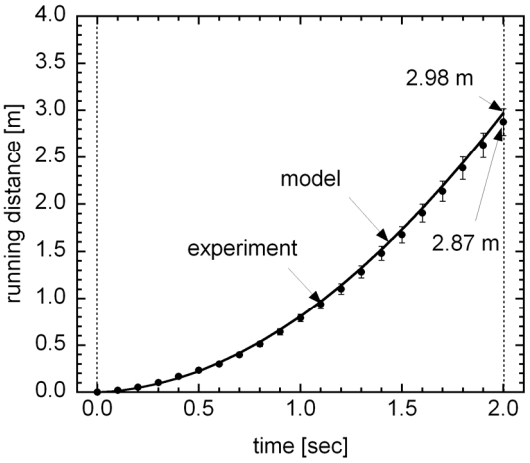

Fig.12 Sliding distance of PDR-TODOROKI

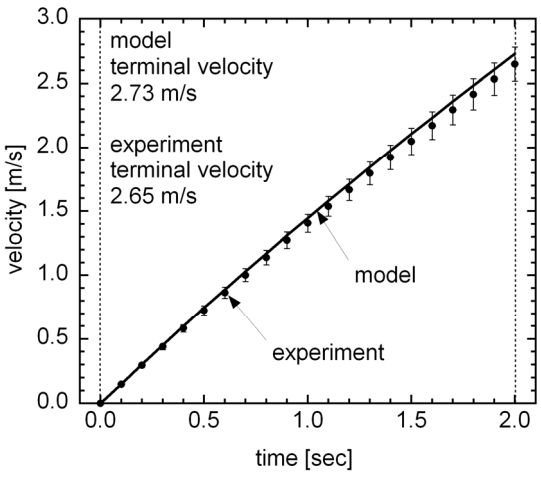

Fig.13 Velocity history of PDR-TODOROKI

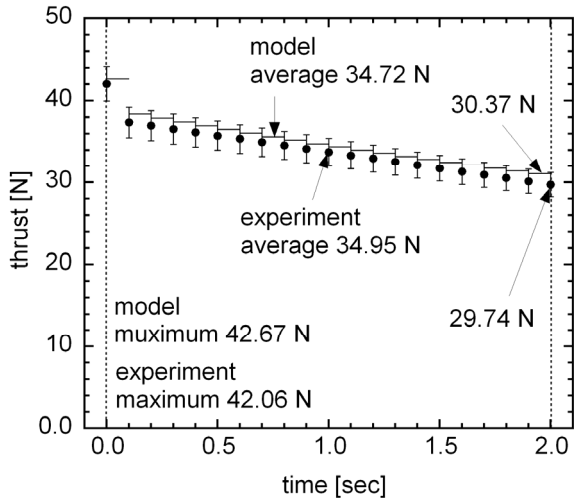

Fig.14 Thrust history of PDR-TODOROKI